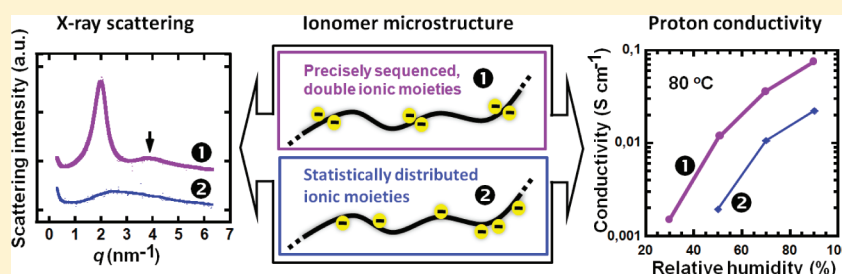


## Fully Aromatic Ionomers with Precisely Sequenced Sulfonated Moieties for Enhanced Proton Conductivity

Xue-Feng Li,<sup>†,‡</sup> François P. V. Paoloni,<sup>†</sup> E. Annika Weiber,<sup>†</sup> Zhen-Hua Jiang,<sup>‡</sup> and Patric Jannasch<sup>†,\*</sup><sup>†</sup>Polymer & Materials Chemistry, Department of Chemistry, Lund University, P.O. Box 124, SE-221 00 Lund, Sweden<sup>‡</sup>Alan G. MacDiarmid Institute, Department of Chemistry, Jilin University, Qianjin Street 2699, Changchun 130012, People's Republic of China

## S Supporting Information



**ABSTRACT:** A series of six fully aromatic ionomers with precisely sequenced sulfonated sites along the polymer chains have been designed, prepared, and characterized as proton-exchange membranes. Two straightforward and efficient synthetic strategies based on Ullmann ether reactions and a Baeyer–Villiger rearrangement were devised to obtain bisphenol monomers with four or six phenylene units linked exclusively by ether bridges to avoid transesterification reactions. Polycondensations of these bisphenol monomers with mono- or disulfonated dihalide monomers gave high molecular weight poly(arylene ether), poly(arylene ether sulfone), and poly(arylene ether ketone) homopolymers having microblock-like structures with sulfonated moieties separated by monodisperse nonsulfonated oligo(ether) spacers. The nanoscale morphology and properties of solvent cast membranes were closely related to the nature of the oligo(ether) spacers. Small angle X-ray scattering (SAXS) measurements showed intense scattering and very narrow ionomer peaks with second-order features for the polymers with the six-ring spacers. This clearly indicated that the controlled ionic sequencing enabled self-assembly of ionic aggregates with a much higher degree of organization in relation to a corresponding aromatic ionomer with a statistical distribution of the sulfonate groups. At an identical ionic content, the ionomers containing *meta* ether linkages had lower glass transition temperatures than the all-*para* materials, leading to a higher water uptake and proton conductivity of the former ionomers. A membrane with an ion exchange capacity (IEC) of 2.05 mequiv g<sup>-1</sup> and containing exclusively *para* linkages reached the same level of proton conductivity as Nafion at 100% relative humidity (RH), and also had an excellent dimensional stability in boiling water. Under reduced RH, the conductivity of this membrane greatly exceeded that of a membrane based on a statistical copolymer analogue with a similar ionic content.

## ■ INTRODUCTION

Sulfonated aromatic hydrocarbon polymers have attracted attention as potential candidates for membranes applied to the production of electrical power and clean water.<sup>1</sup> For example, sulfonated poly(aryl ether)s represent an attractive alternative to perfluorinated sulfonic acid membranes for high temperature proton-exchange membrane fuel cells (PEMFCs) because of their excellent stability and high glass transition temperature ( $T_g$ ).<sup>2</sup> An increase of the operating temperature to above 100 °C promises crucial benefits concerning the complexity, cost and performance of automotive PEMFC systems.<sup>3,4</sup> However, the performance and durability of fuel cell core components such as the membrane need be further improved to meet the demands of the industry.

Early examples of sulfonated poly(aryl ether)s were primarily obtained by postpolymerization sulfonations.<sup>5,6</sup> Characteristically,

membranes based on these polymers show excessive swelling in water, and even water solubility, at high acid contents, which limits their applicability. Partial sulfonations result in statistical distributions of acid groups along the polymer backbones. Unlike perfluorosulfonic acid membranes, these hydrocarbon membranes do not usually form well-connected water-filled channels that promote efficient transport of protons across the membrane.<sup>7</sup> Similar issues arise when sulfonated poly(aryl ether)s are prepared using a presulfonated monomer. If for example polymers are prepared by polycondensations of a presulfonated dihalide monomer with a conventional similar-sized nonsulfonated diol monomer, the acid groups will be

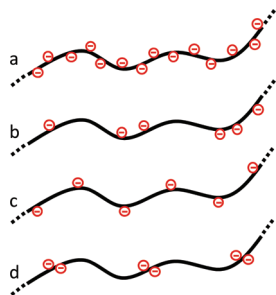
Received: July 13, 2011

Revised: January 4, 2012

Published: January 23, 2012

regularly spaced but the acid content is likely to be too high (Scheme 1). The common strategy is then to use a second non-

**Scheme 1. Schematic Ionomer Structures Illustrating the Distribution of Sulfonic Acid Groups along the Backbone in Regular Homopolymers (a), in Statistical Copolymers (b), and in Homopolymers with Precisely Sequenced Singlet (c) and Doublet (d) Acid Groups**



sulfonated comonomer to form statistical copolymers with reduced acid contents. However, this also leads to an irregular statistical distribution of sulfonic acid along the polymer backbone.

Several research groups have reported that synthetic strategies involving a careful control of the distribution and location of the sulfonic acid groups in the polymer structure result in well-defined hydrocarbon membrane morphologies.<sup>8,9</sup> This may in turn lead to the formation of well-connected water-filled channels which gives the membranes superior proton-conducting properties in relation to statistically sulfonated membranes, particularly at low relative humidity (RH). Mild methods to synthesize sulfonated multiblock copoly(aryl ether sulfone)s have been extensively used by McGrath et al.<sup>10–13</sup> and others.<sup>14–17</sup> Low-temperature coupling of oligomers mediated by a perfluorinated compound such as hexafluorobenzene or decafluorobiphenyl affords high molecular weight multiblock copolymers while limiting the extent of transesterification reaction. These multiblock copolymers typically exhibit quite well-defined morphologies, associated with high proton conductivity under reduced RH.<sup>8,9</sup> The length and acid density of the sulfonated blocks have a major influence on the membrane morphology and properties. This concept has been extended to copolymers which contain densely sulfonated blocks to further improve the membrane properties.<sup>18–23</sup> In another synthetic strategy, high local concentrations of sulfonic acid groups have been placed on pendant chains to form defined morphologies, as shown by small-angle X-ray scattering (SAXS) measurements.<sup>24,25</sup> The results indicated that ionic clustering was promoted by placing the sulfonic acid groups on the relatively long spacers. Increasing the number of sulfonic acid groups located on pendant chains from one to three resulted in larger ionic clusters and narrower ionomer peak widths.<sup>24,25</sup>

Several groups have reported on sulfonated poly(aryl ether)s composed of long hydrophobic segments combined with densely sulfonated units. For example, Hay et al. have prepared polymers containing clusters of up to 12 sulfonic acid groups statistically distributed along the backbone chain.<sup>26</sup> Novel bisphenols having six pendant phenyl groups were incorporated in poly(aryl ether)s by polymerization of carefully chosen comonomers. The bisphenol monomer residues underwent selective multiple sulfonations under mild conditions, resulting in statistical copolymers containing highly sulfonated moieties.

The corresponding membranes had higher proton conductivity than typically observed for randomly sulfonated hydrocarbon membranes or multiblock copolymers with similar acid content.

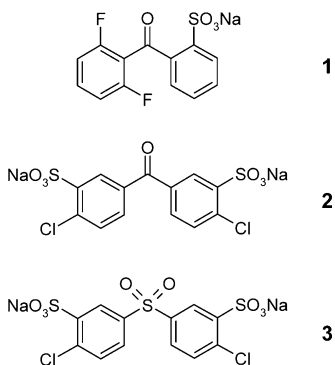
Colquhoun and co-workers have recently prepared and studied microblock ionomers, a novel class of sulfonated poly(aryl ether)s membranes.<sup>27</sup> In these polymers, densely sulfonated moieties are regularly spaced by monodispersed nonsulfonated segments. Essentially, these microblock copolymers are homopolymers with a very large repeat unit. The monomers were designed to yield a repeat unit composed of a long sequence of electron-poor aromatic rings, strictly alternating with a short segment composed of electron-rich phenylene units. Transesterification was avoided by excluding ether linkages activated by a sulfone or ketone bridge. Postpolymerization sulfonation under mild conditions was then selective toward electron-rich aromatic rings. The authors described a series of membranes with an ion exchange capacity (IEC, milliequivalents of H<sup>+</sup> per gram dry membrane) of approximately 2.1 mequiv g<sup>-1</sup>.<sup>27</sup> Although these ionomers show attractive properties, they still suffer from two main drawbacks. First, it is often acknowledged that sulfonic acid groups located next to ether linkages are activated for desulfonation under fuel cell operation.<sup>28,29</sup> Second, the synthesis of the monomers used for the microblock copolymers is limited and quite complex. The monomers must be designed to eliminate the risk of transesterification reactions during the polymerization, and the bisphenol monomers must thus exclusively contain ether linkages. The number of phenylene units in these monomers will essentially determine the degree of sulfonation of the corresponding polymer. The bisphenol monomers exclusively contain ketone or sulfone bridges and are often associated with poor solubility because of the high rigidity of these bonds. In addition, high local acid concentrations in the repeat unit require long dihalide monomers which are not straightforward to synthesize and purify.

In the present study, we have followed an alternative approach to sulfonated microblock poly(aryl ether)s by employing nucleophilic polycondensations of long bisphenols with sulfonated dihalide monomers. The resulting fully aromatic ionomers were composed of long hydrophobic segments, strictly alternating with singlets or doublets of sulfonic acid groups, as illustrated in Scheme 1. First, efficient methods to prepare various novel oligomeric bisphenol monomers were developed. In these monomers, the phenylene rings were exclusively connected by ether bridges in the *meta* or *para* position. Their polymerization with three different sulfonated monomers afforded six homopolymers. Two of these were composed of singlets of sulfonic acid precisely sequenced by a monodisperse oligo(ether) segment of exactly four phenylene units. The remaining four homopolymers were composed of doublets of sulfonic acid precisely sequenced by a monodisperse oligo(ether) segment of exactly six phenylene units. Solvent cast membranes were characterized with regard to ionic distribution, water uptake, thermal stability, and proton conductivity. Special attention was given to the polymer backbone structure, acid group distribution, nanostructure, and influence on the membrane properties.

## ■ RESULTS AND DISCUSSION

**Synthesis of Sulfonated Monomers.** The sulfonated monomers prepared and used in the present work are shown in Scheme 2. These monomers can take part in nucleophilic polycondensation via displacement of the chlorine or fluorine

Scheme 2. Sulfonated Monomers Used in the Present Study



atoms which are activated by an electron-withdrawing ketone or sulfone link. By employing presulfonated monomers, it is possible to accurately control the location of the sulfonic acid groups in the resulting polymers.

The lithium salt of 2,6-difluoro-2'-sulfo-1,1'-biphenyl-4,4'-dicarbonyl (1) was conveniently synthesized in one-pot by reacting 2,6-difluorophenyllithium with 2-sulfo-1,1'-biphenyl-4,4'-dicarbonyl in tetrahydrofuran (THF) at  $-70\text{ }^{\circ}\text{C}$ .<sup>30</sup> After reaction, the product readily crystallized out of solution. We have recently reported that the polymerization of this monosulfonated monomer with various bisphenols and bithiophenols proceeds with a high reaction rate to produce corresponding high molecular weight poly(arylene ether)s.<sup>30</sup> 3,3'-Disulfonated-4,4'-difluorobenzophenone (2)<sup>31</sup> and 3,3'-disulfonated-4,4'-dichlorodiphenyl sulfone (3)<sup>32,33</sup> were synthesized via well-known procedures. The use of sulfonated monomers readily ensures reproducibility of the degree of sulfonation. Moreover, the side reactions and degradation<sup>5</sup> that are sometimes observed for sulfonation under harsh conditions are avoided. In addition, it is recognized that sulfonated polymers are most stable toward desulfonation when the sulfonic acid groups are located on electron-poor aromatic rings. The IEC of the homopolymers containing monomer 1, 2, or 3 can conveniently be controlled by employing monodisperse bisphenol monomers of varying molecular weight. In the case of monomer 1, this will result in single sulfonic acid groups regularly spaced along the polymer backbone (Scheme 1c). The ionomers based on monomers 2 or 3 will consist of doublets of sulfonic acid groups, strictly alternating with hydrophobic segments (Scheme 1d).

**Synthesis of Bisphenol Monomers.** The bisphenol monomers will form monodisperse hydrophobic segments once incorporated in the polymer. This will result in a distribution of sulfonic acid groups that is controlled with molecular precision. As mentioned above, it is imperative that the bisphenol monomers do not contain any electron-withdrawing groups in order to exclude the possibility of transesterification during the polymerizations. Indeed, such reactions would result in chain-scrambling and introduction of defects in the sequence of the polymer backbone. Therefore, the bisphenol monomers were designed to contain aromatic rings linked exclusively by ether bonds or direct aryl-aryl bonds.

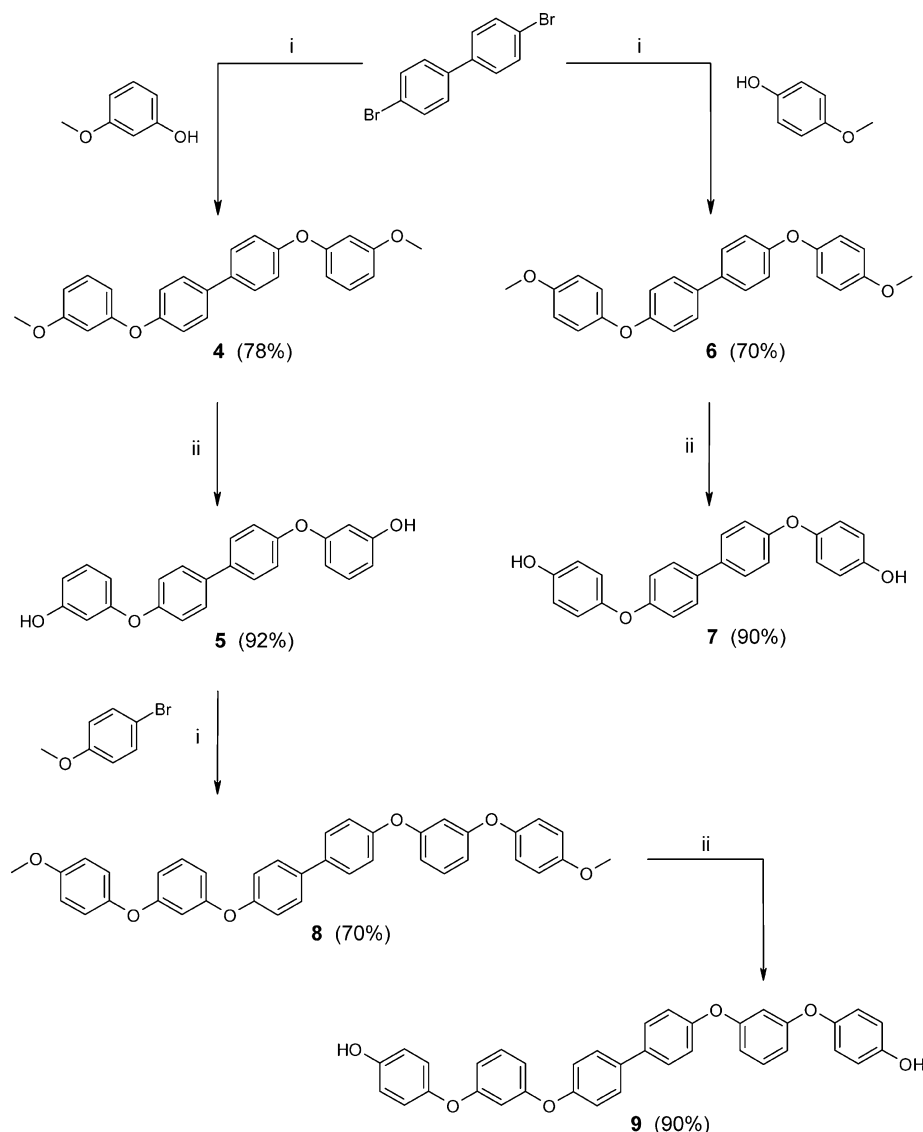
Two bisphenol monomers composed of four aromatic rings (5 and 7) were obtained by Ullmann ether condensation followed by hydrolysis of the methoxy protecting groups, as shown in Scheme 3. Thus, the reaction of 4,4'-dibromobiphenyl with 3-methoxyphenol gave the methoxy-terminated four-ring monomer precursor 4 in good yield. This precursor was

efficiently isolated and purified by filtration through Celite to remove the copper catalyst, followed by precipitation in methanol. The highest yields were obtained under the conditions described by Song and co-workers.<sup>34</sup> Notably, the reaction of 4,4'-bisphenol and 1-bromo-3-methoxybenzene under identical conditions gave 4 in poor to moderate yield only. The methoxy groups of 4 were hydrolyzed by using hydrobromic acid in acetic acid, and bisphenol monomer 5 was isolated by precipitation in water and then washed extensively to remove traces of acids. The product was purified by recrystallization from hot toluene and isolated in 72% overall yield. Complete removal of the methyl groups was confirmed by the total disappearance of the resonance corresponding to the methyl group at 3.81 ppm in the  $^1\text{H}$  NMR spectrum (the  $^1\text{H}$  NMR spectra of all the bisphenol monomers of the present study, and their respective intermediates, are shown in the Supporting Information). The complete removal was further confirmed by the absence of resonances in the aliphatic region of the  $^{13}\text{C}$  NMR spectrum. Formation of the phenol was finally also supported by the presence of a broad absorption band centered at  $3357\text{ cm}^{-1}$  in the FT-IR spectra. The synthetic strategy described above is attractive because of the large variety of aromatic building blocks available and because of its simplicity. Therefore, additional bisphenol monomers with varying length and connectivity can be envisaged. Monomer 7 was synthesized in good yield by an identical method. Ullmann ether condensation of 4,4'-DBBP (4,4'-dibromobiphenyl) and 4-methoxyphenol, followed by hydrolysis of methoxy protecting groups, gave a four-ring bisphenol monomer with *para* connectivity. As expected, the connectivity had an influence on the melting point of these oligomers, and bisphenol 7 had a higher melting point ( $249\text{ }^{\circ}\text{C}$ ) than bisphenol 5 ( $168\text{ }^{\circ}\text{C}$ ). As a result, the former monomer was not soluble in chloroform and appeared to generally have a lower solubility than the latter.

The two-step method described above was also adapted to attempt the synthesis of longer bisphenol oligomers. Reaction of 5 with 4-bromoanisole gave a bismethoxy terminated oligomer 8. Its hydrolysis with HBr afforded a six-ring oligo(ether) monomer 9 that contained both *meta* and *para* linkages. Monomer 9 was obtained in 63% yield over two steps after purification by recrystallization from hot toluene. The structure was confirmed using the same analytical techniques as mentioned previously. The monomer had a melting point similar to the shorter *meta* monomer 5. Unfortunately, the reaction of 5 with 3-bromoanisole gave a mixture of products. Analysis by  $^1\text{H}$  NMR spectroscopy indicated that the main component was the desired all-*meta* oligomer. However, it was not possible to isolate the target compound by precipitation and filtration. In addition, the reaction of 6 with 4-bromoanisole did not afford the targeted six-ring oligomers. Analysis by  $^1\text{H}$  NMR spectroscopy suggested that the reaction was mostly limited to a monosubstitution that produced an oligomer composed of five aromatic units.

An alternative route involving a condensation followed by a Baeyer-Villiger oxidation<sup>35</sup> was utilized in order to synthesize an all *para* oligomer with six rings. As shown in Scheme 4, the reaction of bisphenol 7 with 4-fluoroacetophenone gave the six-ring oligomer 10. In this case the fluorine atom is activated toward nucleophilic aromatic substitution by the ketone in *para* position, resulting in a higher conversion than for the Ullmann ether condensation. The oligomer was insoluble in both chloroform and dimethyl sulfoxide (DMSO). Consequently, it was characterized by NMR spectroscopy using a mixture of

Scheme 3. Synthesis of Four-Ring Bisphenol Monomers **5** and **7** and Six-Ring Monomer **9** by Ullmann Ether Condensation Followed by Hydrolysis of the Methoxy End Groups<sup>a</sup>



<sup>a</sup>Key: (i)  $\text{CuCl}$ ,  $\text{Cs}_2\text{CO}_3$ , THMD, NMP,  $165^\circ\text{C}$ ; (ii)  $\text{HBr}$ ,  $\text{AcOH}$ ,  $150^\circ\text{C}$ .

$\text{CDCl}_3$  and trifluoroacetic acid. This solvent mixture is known to be a good solvent for the solubilization of fully aromatic poly(ether ketone)s.<sup>36–39</sup>

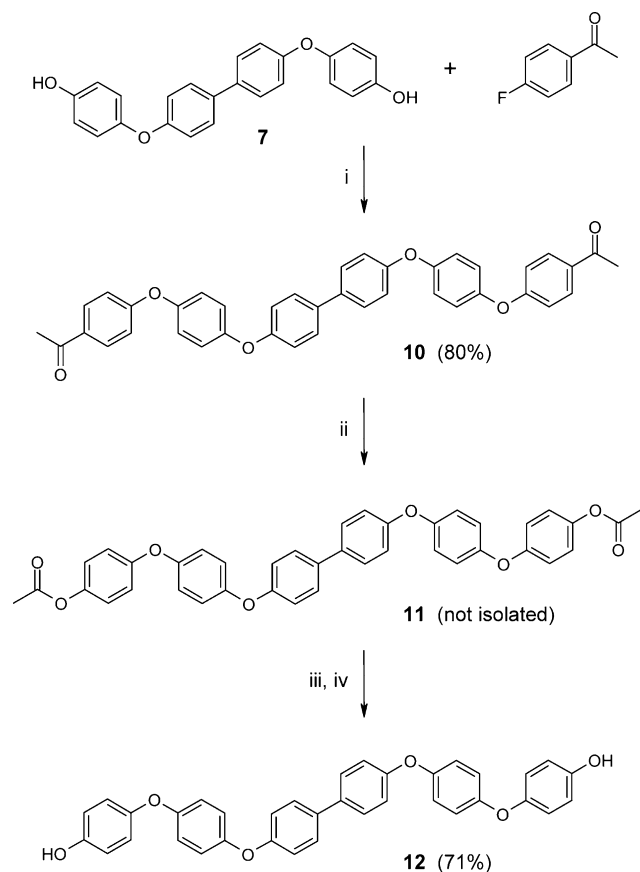
Aromatic–aliphatic ketones can be converted to arylate esters by Baeyer–Villiger rearrangements.<sup>40</sup> The conversion of the reaction with *m*CPBA (*m*-chloroperbenzoic acid) in chloroform was limited, even when a large excess of reactant was used because of the poor solubility of **10**. Poly(ether ketone)s can undergo homogeneous chemical modification in a mixture of chlorinated solvent and TFA (trifluoroacetic acid).<sup>36–39</sup> In the case of Baeyer–Villiger rearrangements, addition of a small amount of TFA has been shown to improve the conversion and to increase the reaction rate. The reaction was monitored by  $^1\text{H}$  NMR spectroscopy through the progressive disappearance of the resonance at 2.73 ppm corresponding to methyl group next to the ketone, and the simultaneous appearance of a singlet at 3.63 ppm originating from the methyl ester. Excess *m*CPBA and TFA were removed by liquid extraction and oligomer **11** was immediately converted to bisphenol

monomer **12** by hydrolysis. The bisphenol monomer was purified by dissolving the crude product in DMF (dimethylformamide), followed by addition of 2-propanol until a cloudy mixture was obtained. Then, the mixture was heated to give a clear solution and bisphenol **12** was recovered as a fine powder upon cooling. This monomer had the highest melting point of the series reported in the present study ( $274^\circ\text{C}$ ).

**Polycondensation and Polymer Characterization.** The six sulfonated homopolymers shown in Scheme 5 were synthesized by polycondensation via nucleophilic aromatic substitutions. The monomers used for each polymer are indicated in Table 1. As seen, the polymers (ionomers) differed with regard to the connectivity and length of the hydrophobic ether segment, and the nature of the sulfonated unit.

Polymers **13** and **14** were prepared by condensation of the monosulfonated monomer **1** with bisphenol monomer **5** and **7**, respectively. These polymers contained singlets of sulfonic acid groups regularly separated by a four aromatic ring spacer, giving them a theoretical IEC of  $1.5 \text{ mequiv g}^{-1}$ . In our previous

**Scheme 4. Synthesis of Bisphenol Monomer 12 by Nucleophilic Aromatic Substitution, Followed by Baeyer–Villiger Rearrangement<sup>a</sup>**



<sup>a</sup>Key: (i)  $K_2CO_3$ , DMF, 150 °C; (ii) *m*CPBA, TFA,  $CHCl_3$ ; (iii) KOH, MeOH; (iv) HCl,  $H_2O$ .

reports on monomer 1, polymerizations with bisphenols were carried out in dimethylacetamide (DMAc).<sup>41,42</sup> In the present case, the polymerizations were carried out in DMSO at 160 °C. After a 4 h dehydration period, the viscosity of the polymerization solution increased significantly after 4 and 6 h, respectively. This suggested that the polymerization of 1 with bisphenols proceeded at a higher rate in DMSO than in DMAc. Furthermore, no precipitation of the polymer was observed.

Next, four polymers were prepared by polycondensations of the six-ring bisphenol monomers 9 and 12 with the disulfonated monomers 2 and 3. The resulting polymers were thus composed of doublets of sulfonic acid groups regularly separated by spacers containing six nonsulfonated aromatic units. The poly(arylene ether ketone)s 15 and 17 had a theoretical IEC slightly higher than the poly(arylene ether sulfone)s 16 and 18. Indeed, monomer 2 has a lower molecular weight than monomer 3. There are many examples of statistical copolymers of similar IEC values prepared from the sulfonated monomers 2 and 3.<sup>8,9</sup> However, to the best of our knowledge, samples 15–18 are the first examples of such homopolymers with an IEC of approximately 2 mequiv  $g^{-1}$ . Polymers 15 and 17 were prepared in DMSO while polymers 16 and 18 were prepared in DMAc. Again, no precipitation of the polymers was observed during the polycondensations.

Figure 1 shows the  $^1H$  NMR spectra of all polymers prepared in this study. In every case, resonances were observed exclusively in the aromatic region. The compositions of the polymers obtained by integrating and comparing the NMR signals were very close to the theoretical values predicted from the monomer feed ratios. Additional spectroscopic data were consistent with the proposed structures. The inherent viscosity ( $\eta_{inh}$ ) of the polymers indicated that moderate to high molecular weights were systematically obtained.<sup>43</sup> Notably, the poly(arylene ether ketone)s 15 and 17 had significantly higher inherent viscosity than the other polymers (Table 1). This might suggest that monomer 3 was more efficient in the polycondensations than monomer 2.

**Membrane Preparation.** Flexible transparent films with a thickness between 70 and 90  $\mu m$  were obtained by casting the polymers from DMAc solutions in all cases but for polymer 18. According to the inherent viscosity measurements, this polymer had a similar molecular weight as the other polymers prepared in the present work. Attempts to prepare thin films from NMP solution at different temperatures and using different casting substrates such as glass and Teflon were unsuccessful. A fragile film was obtained in every case and thus it was not possible to further evaluate the membrane properties of polymer 18. As seen in Table 2, the IEC values of the other membranes were in very good agreement with the theoretical value calculated from the monomer feed ratios. This again confirmed the structure of the polymers prepared.

**X-ray Scattering.** The morphological features of the completely amorphous ionomer membranes were studied by SAXS measurements. Generally, a broad scattering peak is observed at scattering vector ( $q$ )  $\approx 1\text{--}5\text{ nm}^{-1}$  in ionomers and is referred to as the “ionomer peak”. This feature is widely attributed to interaggregate scattering and its position ( $q_{max}$ ) can be correlated to the characteristic separation length ( $d$ ) between the ionic aggregates in the polymer-rich matrix phase.<sup>44</sup> Because this scattering feature is usually relatively broad and weak, intraparticle interference have also been proposed to give rise to the ionomer peak.<sup>45</sup> However, there is now a general consensus in the community that the scattering originates from interaggregate scattering.

Shown in Figure 2 are the SAXS profiles of ionomers 13 and 14, based on the four-ring bisphenols, and ionomers 15–17, based on the six-ring bisphenols. Before analysis, the membranes were ion-exchanged to selectively stain the sulfonated domains of the membranes with  $Pb^{2+}$  to enhance the contrast. The values of  $q_{max}$  and  $d$  are collected in Table 2 for membranes 13–17. For comparison, the corresponding data of Nafion NRE212 (IEC = 0.91 mequiv  $g^{-1}$ ) and an archetypical post-polymerization sulfonated aromatic polymer, poly(phenylsulfone) (sPPSU), are included in the  $Pb^{2+}$  form. The latter polymer was obtained by polycondensation of 4,4'-biphenol and 4,4'-dichlorodiphenyl sulfone, followed by sulfonation using sulfuric acid. The fully aromatic sPPSU had an IEC of 1.84 mequiv  $g^{-1}$  and a backbone with similar structural elements as ionomers 15–17, but with the sulfonic acid units statistically distributed along the polymer backbone in *ortho*-ether positions (Scheme 6). As seen in Figure 2, the ionomer peak of the sPPSU membrane was much broader and shifted toward a higher  $q$ -value ( $q_{max} = 2.4\text{ nm}^{-1}$ ), as compared to the profile of the Nafion membrane ( $q_{max} = 1.65\text{ nm}^{-1}$ ). The values of  $q_{max}$  corresponded to  $d = 1.65\text{ nm}$  for sPPSU and 3.8 nm for Nafion. The results thus indicated a smaller average interaggregate distance with a wider distribution in the sPPSU membrane. The extremely hydrophobic

**Scheme 5. Ionomers Having Poly(arylene ether) (13 and 14), Poly(arylene ether ketone) (15 and 17) and Poly(arylene ether sulfone) (16 and 18) Backbones with Precisely Sequenced Ionic Moieties**

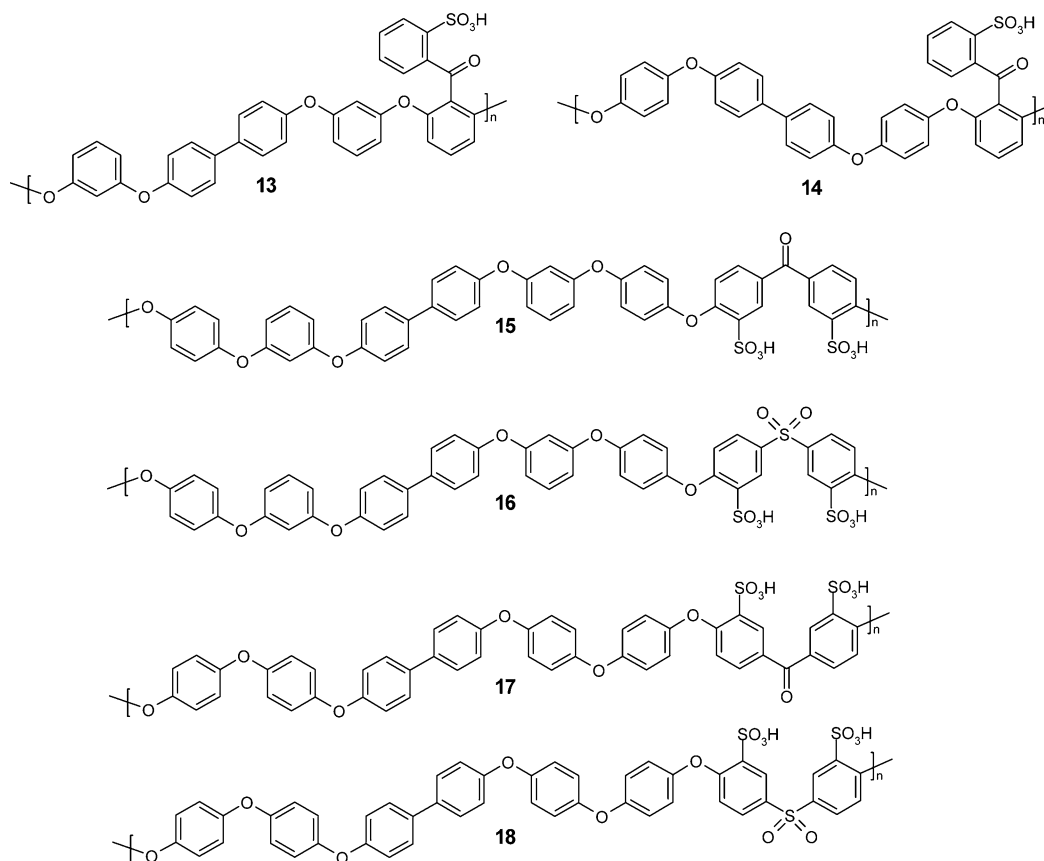


**Table 1. Properties of Sulfonated Homopolymers**

polymer	sulfonated monomer	bisphenol monomer	$\eta_{inh}$ (dL g <sup>-1</sup> ) <sup>a</sup>	$T_g$ (°C) <sup>b</sup>
13	1	5	0.35	230
14	1	7	0.24	259
15	2	9	0.47	304
16	3	9	0.20	283
17	2	12	0.51	348
18	3	12	0.29	302

<sup>a</sup>0.5 wt % in DMF containing LiBr (0.05 M) at 25 °C. <sup>b</sup>Measured for polymers in the Na<sup>+</sup> form.

polymer backbone combined with the superacidity and hydrophilicity of the  $-\text{CF}_2-\text{SO}_3\text{H}$  unit in Nafion give rise to a distinct phase separation and a quite well-defined morphology. Typically, aromatic hydrocarbon backbones are far less hydrophobic and the arylenesulfonic acid units of these ionomers are far less acidic, which leads to a morphology with a less pronounced phase separation. The morphological differences between Nafion membranes and statistically sulfonated aromatic hydrocarbon membranes have previously been extensively discussed by Kreuer on the basis of SAXS data.<sup>7</sup>

The SAXS profiles of membranes 13 and 14 showed ionomer peak positions at higher  $q_{\max}$  in comparison with sPPSU. Moreover, the peaks were significantly narrower, with membrane 14 showing the narrowest one. Seemingly, the structure of 13 and 14 with monosulfonated sites spaced by four-ring oligo(ether) segments decreased the distributions of

the interaggregate distances in relation to the statistical copolymer.

It is immediately clear from Figure 2 that membranes 15–17 gave rise to dramatically different scattering profiles with considerably more intense scattering and much narrower ionomer peaks than both sPPSU and Nafion. The value of  $q_{\max}$  for these ionomer membranes was approximately the same as for Nafion, approximately 2 nm<sup>-1</sup>. Apparently, by precisely controlling the acid group separation, and keeping it sufficiently large, the ionomer peak became much more intense and well-defined. A further strong indication of the narrow distribution in the interaggregate correlation length was the appearance of clear second order-peaks at  $2q_{\max}$  (indicated by arrows in Figure 2). These were similar in appearance to those only previously observed in the scattering profiles of monodisperse halato telechelic ionomers<sup>46</sup> and other well-defined model ionomers.<sup>47,48</sup> To our knowledge, this is the first report on second-order features observed for fully aromatic ionomers. There was seemingly no influence by the connectivity of the oligo(ether) spacers and the sulfonated moieties (sulfone or ketone) on the scattering peak position and width of ionomers 13–17. Obviously, the precise ionomers with their evenly and sufficiently spaced ionic moieties allowed for a much more uniform self-aggregation of the ionic groups to occur. This in turn indicated an increased degree of phase separation and morphological control of the membranes. Previously, Colquhoun and co-workers have studied the morphology of microblock polymers with sulfonated moieties precisely spaced by oligo(arylene ketones) by SAXS.<sup>27</sup> They observed that a polymer

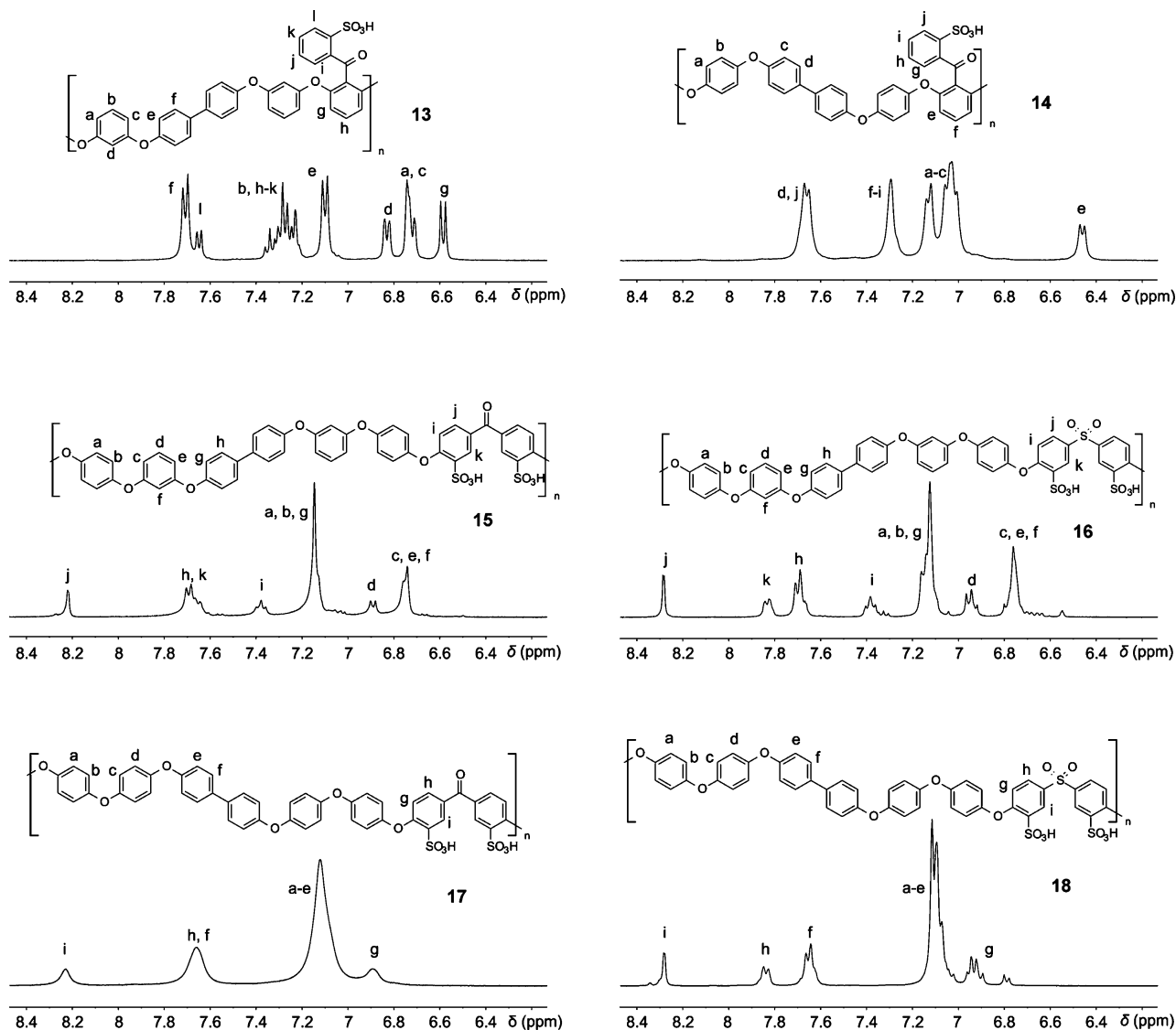


Figure 1.  $^1\text{H}$  NMR spectra ( $\text{DMSO}-d_6$ ) of the precisely sequenced sulfonated polymers, identified by their numerals.

Table 2. Properties of the Ionomer Membranes

polymer	theoretical IEC ( $\text{mequiv g}^{-1}$ )	titrated IEC ( $\text{mequiv g}^{-1}$ )	$q_{\text{max}}$ ( $\text{nm}^{-1}$ ) <sup>a</sup>	$d$ (nm) <sup>a</sup>	$T_{95-\text{Na}}$ ( $^{\circ}\text{C}$ ) <sup>b</sup>	$T_{95-\text{H}}$ ( $^{\circ}\text{C}$ ) <sup>c</sup>	water uptake (wt %)	$\lambda$
13	1.50	1.50	2.8	2.2	398	292	22	8.1
14	1.50	1.48	2.6	2.4	404	171	28	10.5
15	2.14	2.06	2.0	3.2	415	305	50	13.5
16	1.99	1.84	1.9	3.3	424	292	68	20.5
17	2.14	2.05	2.0	3.2	442	296	44	11.9

<sup>a</sup>Membranes in the  $\text{Pb}^{2+}$  form. <sup>b</sup>Temperature corresponding to a 5% weight loss of membranes in their  $\text{Na}^+$  form under nitrogen atmosphere at a heating rate of  $10\text{ }^{\circ}\text{C min}^{-1}$ . <sup>c</sup>Temperature corresponding to a 5% weight loss of membranes in their protonated form under air at a heating rate of  $1\text{ }^{\circ}\text{C min}^{-1}$ .

with six-ring spacers showed a small but well-defined peak, indicating scattering at the same length-scale as that observed for Nafion. A polymer with 12-ring spacers showed a very much more intense peak, at significantly lower  $q$ , than for the one with the six-ring spacers, thus showing similar trends as observed in the present work. However, Colquhoun et al. found no second-order scattering features of their membranes. Possibly, the higher mobility of the oligo(ether) segments in relation to the oligo(ketone) segments allowed for a more

efficient ionic aggregation in the present case. We have previously shown that membranes based on poly(arylene ether sulfone)s with sulfonic acid groups on short side chains gave SAXS profiles with narrow ionomer peaks at lower  $q_{\text{max}}$  than corresponding polymers with sulfonic acid groups statistically distributed along the backbone.<sup>24,25</sup> However, in this case no second order features were found.

The nature of the counterion have previously been reported to influence the morphology of ionomers.<sup>49</sup> In order to

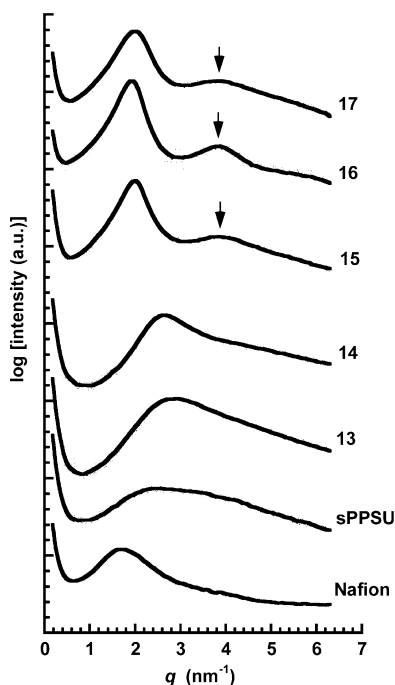
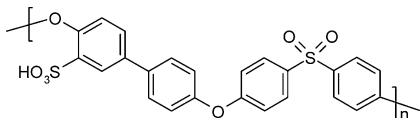


**Figure 2.** SAXS data recorded using ionomer membranes ion-exchanged with lead acetate to enhance the scattering intensity. The arrows indicate second-order peaks at  $2q_{\max}$ .

**Scheme 6. Structure of the sPPSU Reference Ionomer with Statistically Sequenced Ionic Groups**



investigate the effect of the counterion in the present case, membranes **13** and **15** were ion-exchanged from their  $\text{Pb}^{2+}$  form to their  $\text{H}^+$  and  $\text{Na}^+$  form, respectively, to study the effect on the SAXS profiles. As seen in Figure 3, the position of the ionomer peak was not significantly influenced by the nature of the counterion. The reason may be that the initial membrane morphology, which is formed during the casting process, is largely retained during the ion-exchange process because of the glassy oligo(ether) segments. Perhaps a larger effect of the counterion would be observed if the membranes had been cast directly from ionomers in different ionic forms. In particular, for the series based on membrane **13**, the scattering intensity decreased with the size of the counterion. In the case of membrane **15**, the intensity of the ionomer peak did not change appreciably with the nature of the counterion. However, the intensity of the second order-peak at  $2q_{\max}$  decreased. It was only very slightly visible for the membrane in the  $\text{Na}^+$  form and had disappeared for the membrane in the  $\text{H}^+$  form.

The thermal history of ionomer membranes cast from high- $T_g$  polymers can be expected to greatly influence the aggregation of ionic groups.<sup>50</sup> To study the effect of annealing on the membranes in the present case, membranes **13** and **15** in the  $\text{Pb}^{2+}$  form were kept at a temperature 20 °C above their respective  $T_g$  (Table 2). The SAXS profiles of the annealed membranes are shown together with the nonannealed (as cast) ones in Figure 4. As seen, the ionomer peak position of

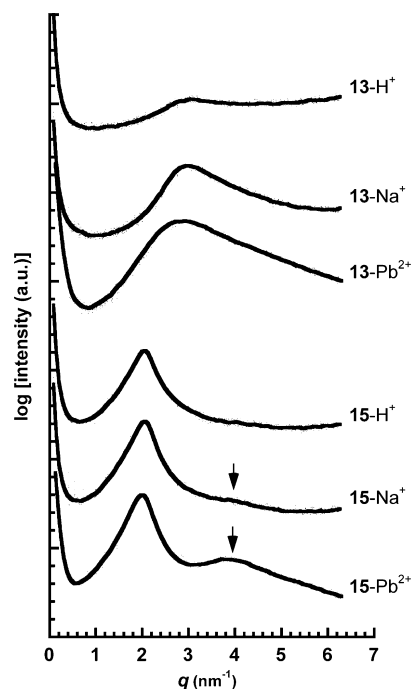


**Figure 3.** SAXS data recorded of ionomer membranes **13** and **15** in the  $\text{H}^+$ ,  $\text{Na}^+$ , and  $\text{Pb}^{2+}$  form, respectively.

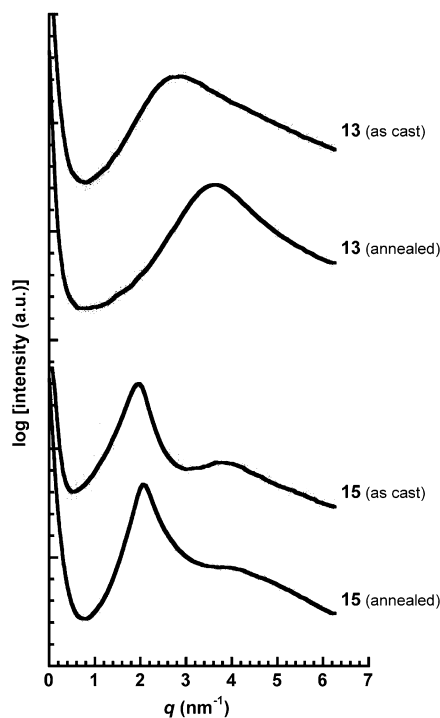


**Figure 4.** SAXS data of membranes **13** and **15** in the  $\text{Pb}^{2+}$  form recorded before (as cast) and after 10 min annealing 20 °C above the respective  $T_g$ .

membrane **13** increased significantly from  $q_{\max} = 2.8$  to  $3.6 \text{ nm}^{-1}$ , corresponding to a decrease in  $d$  from 2.2 to 1.7 nm. On the other hand, membrane **15** was only slightly affected by the annealing and the ionomer peak position decreased only very slightly,  $0.1 \text{ nm}^{-1}$ . This indicated that ionomer **15** with its doublet ionic moieties and longer oligo(ether) segments

reached closer to an equilibrium structure during the casting process.

**Thermal Properties.** The thermal stability of the membranes was evaluated by thermogravimetric analysis (TGA) up to 600 °C. Measurements were performed at 10 °C min<sup>-1</sup> under N<sub>2</sub> with the membranes in their Na<sup>+</sup> form. In addition, measurements were done at 1 °C min<sup>-1</sup> under air with the membranes in their acid form to investigate the oxidative stability of the materials under more drastic conditions. The TGA traces are shown in Figure 5 and the

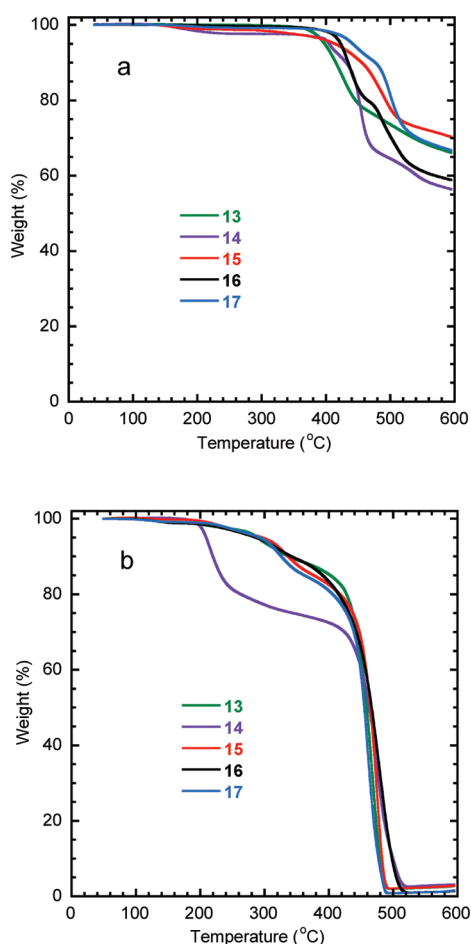


**Figure 5.** TGA traces of the sulfonated membranes in their Na<sup>+</sup> form recorded at 10 °C min<sup>-1</sup> under nitrogen (a), and their acid form recorded at 1 °C min<sup>-1</sup> under air (b).

temperatures corresponding to a 5% weight loss ( $T_{95}$ ) are summarized in Table 2. In the Na<sup>+</sup> form, the polymers containing ether segments with *para* connectivity showed slightly higher  $T_{95}$  values than the corresponding polymers containing *meta* connectivity. Moreover, the polymers containing six-ring ether segments and doublets of acid units had higher  $T_{95}$  values than the polymers containing four-ring ether segments and singlets of acid units. The  $T_{95}$  values of the polymers in the Na<sup>+</sup> form were found between 400 and 442 °C. As expected, the thermal stability decreased after converting the membranes to the acid form. Still, the ionomers had high thermo-oxidative stability as demonstrated by their high  $T_{95}$  values above 290 °C. For some reason ionomer 14 exhibited a drastic weight loss already from 170 °C. A similar degradation has previously been observed in some cases for membranes based on monomer

1.<sup>41,42</sup> For all the polymers, the degradation occurred in two steps, presumably by desulfonation followed by polymer main chain degradation.

Glass transitions were studied by differential scanning calorimetry (DSC) for the polymers in their Na<sup>+</sup> form and the values are found in Table 1 (the DSC traces the membranes in the Na<sup>+</sup> form are shown in the Supporting Information). Glass transitions were not always detected for the polymers in their acid form. However, in the cases where it was found, the  $T_g$  values recorded for the two forms were similar. The polymers containing six-ring ether segments and doublets of acid units showed higher  $T_g$  values than the polymers containing four-ring ether segments and singlets of acid units. As expected for materials based on the same sulfonated monomer, the polymer having an all-*para* connectivity in the hydrophobic polyether segment had a higher  $T_g$  than the corresponding polymer with *meta* connectivity. For example, the  $T_g$  of polymer 14 was 30 °C higher than for 13. Also, for polymers with identical ether segment, ketone monomer 2 gave a higher  $T_g$  than polymers derived with sulfone monomer 3. As a result, the polymer with the highest  $T_g$  in this study was 17. In its Na<sup>+</sup> form, the value was found at 348 °C, close to the degradation temperature.

**Water Uptake and Proton Conductivity.** The water uptake plays a critical role for proton conducting polymer membranes. The presence of water is necessary to facilitate proton transport, and high proton conductivity is often associated with high IECs and high water uptake. However, excessive water uptake leads to loss of dimensional stability of the membrane. The water uptake at room temperature and the corresponding number of water molecules per sulfonic acid group ( $\lambda$ ) are reported in Table 2. The membranes based on the polymers with the four-ring ether segments had an IEC of approximately 1.5 mequiv. g<sup>-1</sup> (13 and 14) and showed lower water uptake values than the membranes based on polymers 15–17 with higher IECs. The latter membranes had water uptakes of between 44 and 68%. The membrane based on polymer 16 had a  $\lambda$  value of 20 which was markedly higher than for the other membranes, which most probably indicated a limited ability of this membrane to resist an excessive water uptake. There was seemingly no clear relationship between polymer chain connectivity and the water uptake at room temperature. However, the polymers containing *meta* linkages in the ether segments all swelled excessively in water at temperatures exceeding 80 °C. Substituting the *meta* linkages by *para* links in the ether segment resulted in a greatly improved dimensional stability of the membrane in hot water. For example, the all-*para* poly(arylene ether ketone) 17 with its high  $T_g$  value did not swell excessively in boiling water.

The proton conductivity of the membranes was evaluated using electrochemical impedance spectroscopy (EIS). Measurements were performed as a function of temperature at 100% RH using a 2-probe method, and also as a function of RH at 80 °C using a 4-probe method. Figure 6 shows the data collected as a function of temperature. As seen in Figure 6, the membranes based on polymers 13 and 14 showed a proton conductivity that was almost an order of magnitude lower than the other membranes under 100% RH. This was due to their lower IEC values and water uptake, as discussed above. Membrane 17 showed a conductivity in level with that of Nafion, and the conductivity of membrane 15 and 16 exceeded that of Nafion under these conditions to reach 0.2 S cm<sup>-1</sup> at 80 °C. The polymer connectivity had direct influence on proton conductivity. Consistently, the *meta* homopolymers had a

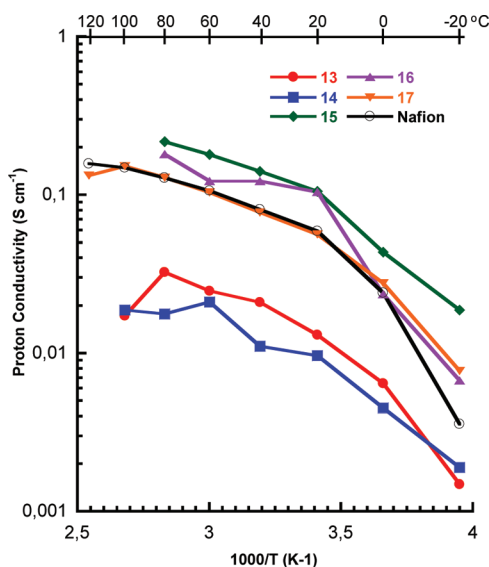


**Figure 6.** Arrhenius conductivity plots of data measured by electrochemical impedance spectroscopy with the membranes under 100% RH in a sealed cell. Values are given for Nafion for comparison.

higher proton conductivity than their *para* analogues. For example, membrane 13 had higher proton conductivity than membrane 14. Similarly, membrane 15 had a higher conductivity than 17. This may be explained by differences in the water uptake and  $T_g$  values. A lower  $T_g$  indicates a higher chain mobility which leads to higher water uptake and conductivity, especially at increasing temperatures.

Figure 7 shows the proton conductivity of 15 and 17 under reduced RH at 80 °C. Included are the corresponding data of

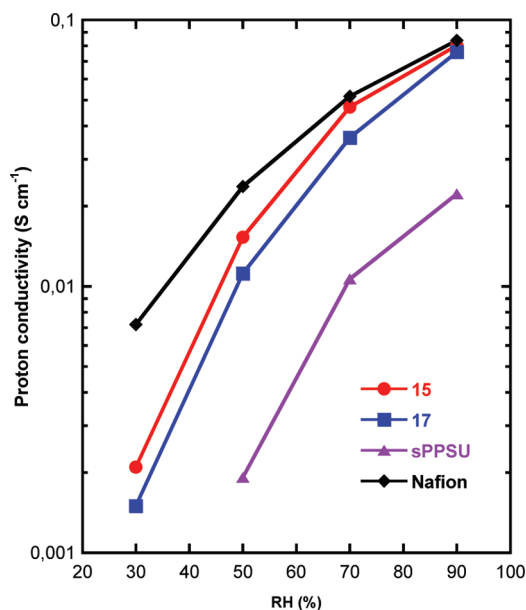


**Figure 7.** Conductivity data measured by electrochemical impedance spectroscopy for membranes 15 and 17 measured at 80 °C under reduced RH. Values for Nafion (IEC = 0.91 mequiv g<sup>-1</sup>) and sPPSU (IEC = 1.84 mequiv g<sup>-1</sup>), with statistically distributed sulfonic acid groups, are given for comparison.

Nafion and sPPSU. As seen, the conductivity of 15 and 17 reached well above that of sPPSU under reduced RH, but fell

below that of Nafion in the investigated range between 30 and 90% RH. Membrane 15 had higher proton conductivity than 17 presumably because of the higher water uptake of the former membrane. The significantly higher proton conductivity of the perfectly sequenced ionic polymer membranes was likely due to the more regular ionic cluster distribution which facilitated the formation of a more efficient water pore system for proton transport.

## EXPERIMENTAL SECTION

**Materials.** Monomer 1,<sup>30</sup> 2,<sup>31</sup> and 3<sup>32,33</sup> were synthesized and characterized as reported previously. Cesium carbonate, magnesium sulfate, Celite, 4,4'-dibromobiphenyl (DBBP), 4-fluoroacetophenone and 4-bromoanisole were obtained from Aldrich. Dimethylformamide (DMF), *N,N*-dimethylacetamide (DMAc), *N*-methyl-2-pyrrolidone (NMP), 2,2,6,6-Tetramethyl-3,5-heptanedione (TMHD), copper(I) chloride, 3-methoxyphenol (*m*MP), 4-methoxyphenol (*p*MP), potassium carbonate, Hydrobromic acid 48%, acetic acid, *m*-chloroperbenzoic acid (*m*CPBA) and trifluoroacetic acid (TFA) were purchased from Acros. Methanol, 2-propanol, diethyl ether, toluene and chloroform were from Fisher. Potassium carbonate was grounded to a fine powder and dried at 120 °C prior to use. Nafion NRE212 was from Alfa Aesar.

**Bismethoxy Oligomer 4.** A setup consisting of a two-neck round bottomed flask heated by an oil bath and equipped with a magnetic stirrer, a N<sub>2</sub> inlet, and a condenser was used in the syntheses. A solution of 4,4'-dibromobiphenyl (1.560 g, 5.00 mmol), Cs<sub>2</sub>CO<sub>3</sub> (1.629 g, 5.00 mmol) 3-methoxyphenol (1.862 g, 15.00 mmol), and 2,2,6,6-tetramethyl-3,5-heptanedione (0.460 g, 2.50 mmol) in NMP (10 mL) was added to the reactor and stirred at room temperature under nitrogen atmosphere. Then CuCl (0.250 g, 2.50 mmol) was added and the mixture was degassed, filled with nitrogen and heated at 165 °C. After 22 h, the solution was cooled, diluted with diethyl ether and filtered through Celite. The filtrate was washed with water, dried with magnesium sulfate, filtered and evaporated. The resulting brown solid was stirred in methanol to afford the desired product 4 that was isolated by filtration as a white powder (1.55 g, 78% yield).

Mp: 104 °C. <sup>1</sup>H NMR (400 MHz, CDCl<sub>3</sub>, δ): 3.81 (6H, s, O-CH<sub>3</sub>), 6.63 (6H, m, Ar), 7.10 (4H, d, Ar), 7.27 (2H, d, Ar), 7.54 (4H, d, Ar). <sup>13</sup>C NMR (100 MHz, CDCl<sub>3</sub>, δ): 55.4, 104.9, 109.1, 111.1, 119.3, 128.2, 130.2, 135.7, 156.3, 158.4, 161.1. IR (KBr): ν<sub>C-H</sub> 3041 cm<sup>-1</sup>, ν<sub>O-CH<sub>3</sub></sub> 2837 cm<sup>-1</sup>, ν<sub>C-O-C</sub> 1128 cm<sup>-1</sup>.

**Bisphenol Monomer 5.** To a stirred solution of 4 (1.99 g, 5.0 mmol) in acetic acid (50 mL) was added 48% HBr (6 mL). After 16 h at 160 °C under air, the solution was cooled and poured in ice. The dark precipitate was washed with water, filtered, and dried under vacuum at 60 °C. Recrystallization in toluene afforded 5 as a brown solid (1.71 g, 92% yield).

Mp: 168 °C. <sup>1</sup>H NMR (400 MHz, CDCl<sub>3</sub>, δ): 6.41 (6H, m, Ar), 7.07 (4H, d, Ar), 7.16 (2H, d, Ar), 7.65 (4H, d, Ar). <sup>13</sup>C NMR (100 MHz, CDCl<sub>3</sub>, δ): 105.9, 109.8, 110.8, 119.6, 128.4, 130.8, 135.1, 156.4, 158.2, 159.3. IR (KBr): ν<sub>C-OH</sub> 3357 cm<sup>-1</sup>, ν<sub>C-H</sub> 3062 cm<sup>-1</sup>, ν<sub>C-O-C</sub> 1128 cm<sup>-1</sup>.

**Bismethoxy Oligomer 6.** A solution of 4,4'-dibromobiphenyl (7.800 g, 25.00 mmol), Cs<sub>2</sub>CO<sub>3</sub> (9.774 g, 30.00 mmol) 4-methoxyphenol (9.310 g, 75.00 mmol), and 2,2,6,6-tetramethyl-3,5-heptanedione (2.302 g, 12.50 mmol) in NMP (50 mL) was stirred at room temperature under nitrogen atmosphere. Then CuCl (1.250 g, 12.50 mmol) was added. The mixture was degassed, filled with nitrogen and heated at 170 °C. After 22 h, the solution was cooled and filtered through Celite. The filtrate was washed with water, dried with MgSO<sub>4</sub> and evaporated. The resulting brown solid was stirred in methanol and the desired product 6 was isolated as a white powder by filtration (6.97 g, 70% yield).

Mp: 210 °C. <sup>1</sup>H NMR (400 MHz, CDCl<sub>3</sub>, δ): 3.82 (6H, s, O-CH<sub>3</sub>), 6.91 (4H, d, Ar), 7.00 (8H, AA'XX', Ar), 7.48 (4H, d, Ar); <sup>13</sup>C NMR (100 MHz, CDCl<sub>3</sub>, δ): 55.3, 114.7, 117.9, 120.8, 127.9,

135.0, 149.9, 157.8. IR (KBr):  $\nu_{\text{C-H}}$  3040  $\text{cm}^{-1}$ ,  $\nu_{\text{O-CH}_3}$  2837  $\text{cm}^{-1}$ ,  $\nu_{\text{C-O-C}}$  1132  $\text{cm}^{-1}$ .

**Bisphenol Monomer 7.** To a stirred solution of **6** (1.394 g, 3.50 mmol) in acetic acid (160 mL) was added 48% HBr (12 mL). The solution was heated to 160 °C for 16 h. Then the solution was poured in ice to give a white precipitate that was filtered and washed with water. The desired product **7** was obtained as a white powder after purification by recrystallization from toluene (1.16 g, 90% yield).

Mp: 249 °C.  $^1\text{H}$  NMR (400 MHz, DMSO- $d_6$ ,  $\delta$ ): 6.79 (4H, d, Ar), 6.91 (8H, AA'XX', Ar), 7.53 (4H, d, Ar).  $^{13}\text{C}$  NMR (100 MHz, DMSO- $d_6$ ,  $\delta$ ): 116.6, 117.6, 121.5, 128.2, 134.1, 148.1, 154.3, 158.2. IR (KBr):  $\nu_{\text{C-OH}}$  3466  $\text{cm}^{-1}$ ,  $\nu_{\text{C-H}}$  3033  $\text{cm}^{-1}$ ,  $\nu_{\text{C-O-C}}$  1132  $\text{cm}^{-1}$ .

**Bismethoxy Oligomer 8.** A mixture of **5** (0.926 g, 2.50 mmol),  $\text{Cs}_2\text{CO}_3$  (1.955 g, 6.00 mmol), 4-bromanisole (1.402 g, 7.50 mmol), and 2,2,6,6-tetramethyl-3,5-heptanedione (0.921 g, 5.00 mmol) were stirred in NMP (7.5 mL) under nitrogen atmosphere. After 30 min, CuCl (0.500 g, 5.00 mmol) was added and the mixture was degassed, filled with nitrogen and heated to 170 °C. After 22 h, the solution was diluted with diethyl ether and filtered through Celite. The filtrate was washed with water, dried with magnesium sulfate, filtered and evaporated. The resulting brown solid was stirred in methanol to afford the desired oligomer **8** that was isolated by filtration (1.01 g, 70% yield).

Mp: 98 °C.  $^1\text{H}$  NMR (400 MHz,  $\text{CDCl}_3$ ,  $\delta$ ): 3.82 (6H, s, O-CH<sub>3</sub>), 6.68 (6H, m, Ar), 6.90 (4H, d, Ar), 7.02 (4H, d, Ar), 7.09 (4H, d, Ar), 7.24 (2H, d, Ar), 7.52 (4H, d, Ar).  $^{13}\text{C}$  NMR (100 MHz,  $\text{CDCl}_3$ ,  $\delta$ ): 55.3, 108.0, 112.1, 112.5, 114.9, 119.2, 120.8, 128.1, 130.3, 135.9, 149.3, 156.0, 158.2, 159.8. IR (KBr):  $\nu_{\text{C-H}}$  3039  $\text{cm}^{-1}$ ,  $\nu_{\text{O-CH}_3}$  2834  $\text{cm}^{-1}$ ,  $\nu_{\text{C-O-C}}$  1122  $\text{cm}^{-1}$ .

**Bisphenol Monomer 9.** To a stirred solution of **8** (1.16 g, 2.0 mmol) in acetic acid (20 mL) was added 48% HBr (5 mL). After 16 h at 160 °C, the solution was poured in ice. The white precipitate was then washed with water, filtered, and dried under vacuum at 60 °C. Recrystallization in toluene afforded the desired product **9** as a red powder (0.99 g, 90% yield).

Mp: 158–166 °C.  $^1\text{H}$  NMR (400 MHz, DMSO- $d_6$ ,  $\delta$ ): 6.54 (6H, m, Ar), 6.77 (4H, d, Ar), 6.92 (4H, d, Ar), 7.09 (4H, d, Ar), 7.30 (2H, d, Ar), 7.64 (4H, d, Ar).  $^{13}\text{C}$  NMR (100 MHz, DMSO- $d_6$ ,  $\delta$ ): 107.5, 112.1, 112.6, 116.6, 119.7, 121.7, 128.5, 131.3, 135.4, 147.7, 154.5, 156.1, 158.2, 160.4. IR (KBr):  $\nu_{\text{C-OH}}$  3384  $\text{cm}^{-1}$ ,  $\nu_{\text{C-H}}$  3068  $\text{cm}^{-1}$ ,  $\nu_{\text{C-O-C}}$  1122  $\text{cm}^{-1}$ .

**Bisacetophenone Oligomer 10.** A solution of monomer **7** (1.111 g, 3.00 mmol), 4-fluoroacetophenone (0.967 g, 7.00 mmol), potassium carbonate (0.967 g, 7.00 mmol) in DMF (10 mL) was stirred at 150 °C under nitrogen atmosphere. After 18 h, the red solution was cooled and poured in water. The resulting white precipitate was filtered, and dried under vacuum at 80 °C (1.454 g, 80% yield).

Mp: 263 °C.  $^1\text{H}$  NMR (400 MHz,  $\text{CDCl}_3/\text{TFA}$  6:1,  $\delta$ ): 2.70 (6H, s, CO-CH<sub>3</sub>), 7.05 (16H, AA'XX', Ar), 7.58 (4H, d, Ar), 8.02 (4H, d, Ar).  $^{13}\text{C}$  NMR (100 MHz,  $\text{CDCl}_3/\text{TFA}$  6:1,  $\delta$ ): 25.6, 116.8, 119.0, 120.5, 122.0, 128.3, 129.9, 131.9, 136.0, 150.2, 154.2, 156.4, 164.1. IR (KBr):  $\nu_{\text{C-H}}$  3043  $\text{cm}^{-1}$ ,  $\nu_{\text{C=O}}$  1678  $\text{cm}^{-1}$ ,  $\nu_{\text{C-C}}$  1600  $\text{cm}^{-1}$ ,  $\nu_{\text{C-O-C}}$  1112  $\text{cm}^{-1}$ .

**Bisphenol Monomer 12.** A suspension of **10** (0.848 g, 1.40 mmol) in chloroform (160 mL) was cooled in an ice bath. Then, *m*CPBA (2.390 g, 10.00 mmol) and trifluoroacetic acid (5 mL) were added successively. The mixture was left to warm up to room temperature and was vigorously stirred in the dark for 72 h. The reaction was then quenched by addition of a saturated solution of  $\text{NaHSO}_3$ . The organic layer was washed with saturated  $\text{NaHCO}_3$  solution and water. It was dried with magnesium sulfate, filtered and evaporated under reduced pressure to give **11** as a white powder. Oligomer **11** was stirred in a 0.1 M solution of KOH in methanol (200 mL) under reflux condition for 90 min. Then the solvent was removed and the resulting residue was suspended in 1 M HCl. The desired bisphenol monomer **12** was isolated by filtration and was purified by adding 2-propanol to a DMF solution until a precipitate was formed. The solid was dissolved by heating and recrystallization from DMF and 2-propanol afforded **12** as a white powder.

Mp: 274 °C.  $^1\text{H}$  NMR (400 MHz, DMSO- $d_6$ ,  $\delta$ ): 6.77 (4H, d, Ar), 6.88 (8H, AA'XX', Ar), 7.01 (8H, AA'XX', Ar), 7.60 (4H, d, Ar).

$^{13}\text{C}$  NMR (100 MHz, DMSO- $d_6$ ,  $\delta$ ): 116.7, 118.5, 119.1, 121.0, 121.2, 134.7, 148.8, 151.3, 154.1, 154.8, 157.3. IR (KBr):  $\nu_{\text{OH}}$  3290  $\text{cm}^{-1}$ ,  $\nu_{\text{C-H}}$  3040  $\text{cm}^{-1}$ ,  $\nu_{\text{C-O-C}}$  1098  $\text{cm}^{-1}$ .

**Polymer 13.** A mixture of potassium carbonate (0.345 g, 2.50 mmol), **5** (0.370 g, 1.00 mmol) and **1** (0.304 g, 1.00 mmol) was suspended in DMSO (3 mL) and toluene (10 mL) in a two-necked flask fitted with a nitrogen gas inlet, a Dean–Stark trap, a condenser and a calcium chloride guard. Water was removed by azeotropic distillation with toluene maintaining a reflux temperature of 140 °C for 4 h. Then, toluene was removed and the reaction temperature was increased to 160 °C. After 4 h the viscous mixture was cooled and poured into 2-propanol. The precipitate was filtered off, washed with water and dried. The solid was dissolved in DMSO and precipitated from 2-propanol to give **13** as a powder that was dried in a vacuum oven at 80 °C.

$^1\text{H}$  NMR (400 MHz, DMSO- $d_6$ ,  $\delta$ ): 6.57 (2H, d, Ar), 6.71 (4H, m, Ar), 6.81 (2H, d, Ar), 7.09 (4H, d, Ar), 7.23 (6H, m, Ar), 7.63 (1H, d, Ar), 7.69 (4H, d, Ar).  $^{13}\text{C}$  NMR (100 MHz, DMSO- $d_6$ ,  $\delta$ ): 110.7, 113.5, 113.8, 114.9, 119.5, 124.4, 127.6, 128.6, 129.1, 129.4, 130.8, 132.4, 135.4, 140.2, 145.5, 156.2, 156.9, 157.7, 158.2, 193.9. IR (KBr):  $\nu_{\text{C=O}}$  1681  $\text{cm}^{-1}$ ,  $\nu_{\text{C-O-C}}$  1089  $\text{cm}^{-1}$ ,  $\nu_{\text{SO}_3}$  1022  $\text{cm}^{-1}$ .

**Polymer 14.** The polymerization of **7** (0.370 g, 1.00 mmol) and **1** (0.304 g, 1.00 mmol) was carried out using an identical procedure as described for polymer **13**. The reaction was stopped after 6 h and **14** was recovered as a white powder.

$^1\text{H}$  NMR (400 MHz, DMSO- $d_6$ ,  $\delta$ ): 6.46 (2H, br, Ar), 7.00 (12H, br, Ar), 7.31 (4H, br, Ar), 7.65 (5H, br, Ar).  $^{13}\text{C}$  NMR (100 MHz, DMSO- $d_6$ ,  $\delta$ ): 112.1, 118.6, 120.7, 121.8, 123.6, 127.7, 128.4, 128.7, 129.3, 132.2, 134.8, 140.4, 145.5, 152.2, 152.7, 157.2, 157.9, 194.1. IR (KBr):  $\nu_{\text{C=O}}$  1683  $\text{cm}^{-1}$ ,  $\nu_{\text{C-O-C}}$  1089  $\text{cm}^{-1}$ ,  $\nu_{\text{SO}_3}$  1019  $\text{cm}^{-1}$ .

**Polymer 15.** A mixture of potassium carbonate (0.207 g, 1.50 mmol), **9** (0.388 g, 0.70 mmol), and **2** (0.296 g, 0.70 mmol) was suspended in DMSO (3 mL) and toluene (10 mL) in a two-necked flask fitted with a nitrogen gas inlet, a Dean–Stark trap, a condenser, and a calcium chloride guard. Water was removed by azeotropic distillation with toluene maintaining a reflux temperature of 140 °C for 4 h. Then toluene was removed and the reaction temperature was increased to 160 °C. After 21 h the viscous mixture was cooled and poured in 2-propanol. The precipitate was filtered off, washed with water and dried. The solid was dissolved in DMSO and precipitated from 2-propanol to give **15** as a powder that was dried in a vacuum oven at 80 °C.

$^1\text{H}$  NMR (400 MHz, DMSO- $d_6$ ,  $\delta$ ): 6.73 (6H, br, Ar), 6.87 (2H, m, Ar), 7.14 (12H, br, Ar), 7.37 (2H, m, Ar), 7.68 (6H, m, Ar), 8.22 (2H, br, Ar).  $^{13}\text{C}$  NMR (100 MHz, DMSO- $d_6$ ,  $\delta$ ): 108.7, 109.0, 112.8, 113.2, 118.1, 119.9, 121.5, 121.7, 122.3, 128.5, 131.1, 131.2, 131.5, 132.6, 135.4, 138.2, 152.3, 152.6, 156.0, 158.4, 159.1, 193.6. IR (KBr):  $\nu_{\text{C=O}}$  1653  $\text{cm}^{-1}$ ,  $\nu_{\text{SO}_3}$  1028  $\text{cm}^{-1}$ .

**Polymer 16.** A mixture of potassium carbonate (0.207 g, 1.50 mmol), **9** (0.388 g, 0.70 mmol) and **3** (0.344 g, 0.70 mmol) was suspended in DMAc (3 mL) and toluene (10 mL) in a two-necked flask fitted with a nitrogen gas inlet, a Dean–Stark trap, a condenser and a calcium chloride guard. Water was removed by azeotropic distillation with toluene maintaining a reflux temperature of 140 °C for 4 h. Then toluene was removed and the reaction temperature was increased to 165 °C. After 22 h the viscous mixture was cooled and poured in 2-propanol. After the purification procedure described above, **16** was recovered as a powder.

$^1\text{H}$  NMR (400 MHz, DMSO- $d_6$ ,  $\delta$ ): 6.76 (6H, br, Ar), 6.91 (2H, m, Ar), 7.12 (12H, m, Ar), 7.36 (2H, m, Ar), 7.68 (4H, m, Ar), 7.82 (2H, m, Ar), 8.28 (2H, br, Ar).  $^{13}\text{C}$  NMR (100 MHz, DMSO- $d_6$ ,  $\delta$ ): 107.6, 109.0, 112.9, 113.2, 116.7, 119.1, 119.9, 121.3, 121.6, 122.3, 128.5, 130.3, 131.3, 131.6, 134.4, 135.5, 139.0, 152.0, 152.7, 155.9, 158.5, 159.0. IR (KBr):  $\nu_{\text{O=S=O}}$  1163  $\text{cm}^{-1}$ ,  $\nu_{\text{SO}_3}$  1027  $\text{cm}^{-1}$ .

**Polymer 17.** A mixture of potassium carbonate (0.207 g, 1.50 mmol), **12** (0.388 g, 0.70 mmol) and **2** (0.296 g, 0.70 mmol) was suspended in DMSO (3 mL) and toluene (10 mL) in a two-necked flask fitted with a nitrogen gas inlet, a Dean–Stark trap, a condenser and a calcium chloride guard. Water was removed by azeotropic distillation with toluene maintaining a reflux temperature of 140 °C for 18 h. The toluene was removed and the reaction temperature was increased

to 160 °C. After 40 min the highly viscous mixture was cooled and poured in 2-propanol. The precipitate was filtered off, washed with water and dried. The solid was dissolved in DMSO and precipitated from 2-propanol to give **17** as a powder that was dried in a vacuum oven at 80 °C.

<sup>1</sup>H NMR (400 MHz, DMSO-*d*<sub>6</sub>,  $\delta$ ): 6.89 (2H, br, Ar), 7.12 (20H, br, Ar), 7.65 (6H, br, Ar), 8.23 (2H, br, Ar). <sup>13</sup>C NMR (100 MHz, DMSO-*d*<sub>6</sub>,  $\delta$ ): 118.1, 118.8, 120.3, 120.5, 121.0, 121.2, 121.3, 122.3, 128.4, 131.1, 132.7, 135.0, 138.2, 152.1, 152.3, 153.3, 153.6, 157.1, 158.7, 193.5. IR (KBr):  $\nu_{\text{C=O}}$  1652 cm<sup>-1</sup>,  $\nu_{\text{SO}_3}$  1027 cm<sup>-1</sup>.

**Polymer 18.** A mixture of potassium carbonate (0.207 g, 1.50 mmol), **12** (0.388 g, 0.70 mmol) and **3** (0.344 g, 0.70 mmol) was suspended in DMAc (3 mL) and toluene (10 mL) in a two-necked flask fitted with a nitrogen gas inlet, a Dean–Stark trap, a condenser and a calcium chloride guard. Water was removed by azeotropic distillation with toluene maintaining a reflux temperature of 140 °C for 4 h. Then toluene was removed and the reaction temperature was increased to 160 °C. After 7 h the mixture was cooled and poured in 2-propanol. Polymer **18** was recovered as a powder after using the same purification as described above.

<sup>1</sup>H NMR (400 MHz, DMSO-*d*<sub>6</sub>,  $\delta$ ): 6.77 (4H, m, Ar), 7.10 (16H, m, Ar), 7.64 (4H, m, Ar), 7.82 (2H, m, Ar), 8.27 (2H, br, Ar). <sup>13</sup>C NMR (100 MHz, DMSO-*d*<sub>6</sub>,  $\delta$ ): 116.7, 118.5, 118.8, 119.0, 120.3, 120.6, 121.0, 121.2, 122.4, 128.5, 130.3, 134.3, 134.9, 138.9, 151.4, 152.4, 153.1, 154.0, 157.1, 159.2. IR (KBr):  $\nu_{\text{O=S=O}}$  1163 cm<sup>-1</sup>,  $\nu_{\text{SO}_3}$  1027 cm<sup>-1</sup>.

**Membrane Casting.** An amount of 0.300 g polymer was dissolved in DMAc (3 mL). The solution was filtered and transferred to a 1 in. Petri dish. Slow evaporation of the solvent at 80 °C under a nitrogen flow afforded transparent membranes that were washed successively with water. The membranes were ion-exchanged to the protonated form by immersion in 1 N HCl for 24 h, followed by leaching with distilled water for 2 days during which time the water was repeatedly exchanged until a neutral pH was reached.

**Polymer Characterization.** <sup>1</sup>H NMR spectra were recorded on a Bruker 400 MHz spectrometer using CDCl<sub>3</sub> or DMSO-*d*<sub>6</sub> solutions of the compounds. Resonances were recorded in  $\delta$  (ppm) and referenced to residual solvent resonances. Fourier-transform infrared (IR) analysis was obtained with a Bruker FS66 spectrometer. Dry polymer samples were ground with potassium bromide and pressed into tablets. Inherent viscosities ( $\eta_{\text{inh}}$ ) were determined at 25 °C for filtered 0.5 wt % polymer solutions in DMF containing 0.05 M LiBr using an Ubbelohde capillary viscometer.

**Membrane Characterization.** Ion exchange capacities (IECs) were determined as follow: a membrane of known weight in its protonated form was immersed overnight in an aqueous solution of sodium chloride. The quantity of protons exchanged was titrated with potassium hydroxide, using phenolphthalein as an indicator. Water uptakes were determined by immersion of membranes in their protonated form in water at room temperature. Differential scanning calorimetry (DSC) was conducted on a TA Instruments Q1000 DSC at a heating and cooling rate of 10 °C min<sup>-1</sup>. Values are reported for the second heating scan of membranes in the Na<sup>+</sup> form. Thermogravimetric analysis was performed on a TA Instruments Q500. Samples were dried at 120 °C before analysis. Thermal stability under nitrogen atmosphere was evaluated for membranes in their Na<sup>+</sup> form at a heating rate of 10 °C min<sup>-1</sup>. Degradation of membranes in their protonated form was assessed at a scanning rate of 1 °C min<sup>-1</sup>. SAXS measurements were carried out on all membranes ion-exchanged to the Pb<sup>2+</sup> form by immersion in a 1 wt % aqueous solution of lead acetate. In addition, membranes **13** and **15** were ion exchanged to their Na<sup>+</sup> and H<sup>+</sup> form to study the effect of the counterion on the scattering. Furthermore, scattering experiments were performed on membranes **13** and **15** (Pb<sup>2+</sup> form) after annealing at 20 °C above their respective *T*<sub>g</sub> for 10 min. All scattering experiments were performed on a SAXSess camera (Kratky, Anton Paar) equipped with a CCD detector. CuK $\alpha$  radiation with a wavelength ( $\lambda$ ) of 0.1542 nm was generated by a PANalytical PW3830 X-ray generator operating at 40 kV and 50 mA. Dry membranes were analyzed in a

solid sample holder at 25 °C. The wave vector (*q*) was calculated by the software (SAXSquant) according to:

$$q = 4\pi\lambda^{-1} \sin(\theta) \quad (1)$$

where  $2\theta$  is the scattering angle. The characteristic separation length (*d*), i.e., the Bragg spacing, was calculated as:

$$d = 2\pi q^{-1} \quad (2)$$

Proton conductivity was measured by electrochemical impedance spectroscopy (EIS) using a Novocontrol V 1.01S dielectric analyzer from -20 to +120 °C under 100% relative humidity. In-plane conductivity was measured using two stainless steel electrodes. Impedance data were collected between 10<sup>-1</sup> and 10<sup>7</sup> Hz at a voltage amplitude of 50 mV. For each temperature, the proton conductivity was taken as the real component of the conductivity corresponding to the minimum of the imaginary component of the conductivity. The humidity dependence of the proton conductivity at 80 °C from 30 to 90% RH was investigated by a four-probe method using a Gamry potentiostat/galvanostat/ZRA and a Fumatech MK3 conductivity cell, where the humidity was equilibrated by deionized water in a closed system.

## CONCLUSIONS

The facile synthesis of a series of new aromatic oligo(ether) bisphenol monomers with four or six phenylene rings enabled the preparation of new ionic aromatic polymers with precisely sequenced ionic moieties having either one or two sulfonic acid groups along the backbone. The fully aromatic polymers thus had a microblock structure and were prepared through conventional polycondensations involving nucleophilic aromatic substitution reactions of one sulfonated dihalide and one bisphenol monomer. The polymers showed quite different properties and morphologies from analogous polymer with statistically placed sulfonic acid groups. SAXS measurements of solvent cast membranes the Pb<sup>2+</sup> form showed that the precise ionomers were able to form ionic aggregates with a much more uniform distribution than a corresponding statistical ionomer with a similar backbone structure. Scattering profiles with very intense scattering, narrow ionomer peaks and second order peaks were observed for the precisely sequenced ionomers having disulfonated moieties and six-ring spacers. This indicated a significantly higher degree of morphological control in relation with the statistical ionomer. No influence of the connectivity of the oligo(ether) spacers and the nature of the sulfonated moieties (sulfone or ketone) on the scattering peak position and width was observed. Thus, ionomers with precisely and sufficiently spaced ionic moieties are required facilitate the highly uniform self-aggregation of the ionic groups. Still, the nature of the connectivity (*meta* vs *para*) of the oligo(ether) influenced the *T*<sub>g</sub>, leading to higher values for the ionomers having *para* connectivity. This in turn led to lower water uptake and proton conductivities of the membranes based on these ionomers. Yet, an ionomer with disulfonated moieties perfectly alternating with a six-ring segment having exclusively *para* linkages reached a proton conductivity similar to Nafion under 100% RH at 80 °C, and had an excellent stability in boiling water. Under reduced RH, the conductivity of this membrane greatly exceeded that of a membrane based on the statistical aromatic copolymer analogue with a similar IEC, especially at low RHs. This was presumably because the more uniform distribution of the ionic aggregates in the membranes based on the precise ionomers facilitated more efficient water channels for proton transport. Even though there is increasing interest in the development of organized

polymer systems such as block copolymers, statistical copolymers are still the class of polymer primarily being used in fuel cells, especially by industry. This is due to the larger number of available synthetic techniques and their ease of synthesis in comparison with complex methods required for block and graft copolymers. Thus, developing efficient synthetic strategies to prepare precisely sequenced fully aromatic ionomers with sufficiently long sequences and appropriate IEC values may be a viable alternative for use as fuel cell membranes with controlled morphology.

## ■ ASSOCIATED CONTENT

### ■ Supporting Information

<sup>1</sup>H NMR spectra of the bisphenol monomers and their intermediates and DSC traces of the membranes in the Na<sup>+</sup> form. This material is available free of charge via the Internet at <http://pubs.acs.org>.

## ■ AUTHOR INFORMATION

### Corresponding Author

\*E-mail: [patric.jannasch@polymat.lth.se](mailto:patric.jannasch@polymat.lth.se). Fax: +46-46-2224012. Telephone: +46-46-2229860.

## ■ ACKNOWLEDGMENTS

We gratefully acknowledge the Swedish Energy Agency for their financial support. Dr. Xuefeng Li wishes to thank the China Scholarship Council. We are also grateful to Shogo Takamuku for the synthesis of the sPPSU sample.

## ■ REFERENCES

- (1) Hickner, M. A. *Mater. Today* **2010**, *13*, 24.
- (2) Iojoiu, C.; Sanchez, J.-Y. *High Perform. Polym.* **2009**, *21*, 673.
- (3) Zhang, J.; Xie, Z.; Zhang, J.; Tang, Y.; Song, C.; Navessin, T.; Shi, Z.; Song, D.; Wang, H.; Wilkinson, D. P.; Liu, Z.; Holdcroft, S. J. *Power Sources* **2006**, *160*, 872.
- (4) Garland, N.; Kopasz, J. J. *Power Sources* **2007**, *172*, 94.
- (5) Iojoiu, C.; Marechal, M.; Chabert, F.; Sanchez, J. Y. *Fuel Cells* **2005**, *5*, 344.
- (6) Jones, D. J.; Rozière, J. J. *Membr. Sci.* **2001**, *185*, 41.
- (7) Kreuer, K. D. *J. Membr. Sci.* **2001**, *185*, 29.
- (8) Higashihara, T.; Matsumoto, K.; Ueda, M. *Polymer* **2009**, *50*, 5341.
- (9) Peckham, T. J.; Holdcroft, S. *Adv. Mater.* **2010**, *22*, 4667.
- (10) Ghassemi, H.; McGrath, J. E.; Zawodzinski, T. A. *Polymer* **2006**, *47*, 4132.
- (11) Roy, A.; Lee, H. S.; McGrath, J. E. *Polymer* **2008**, *49*, 5037.
- (12) Lee, H. S.; Roy, A.; Lane, O.; Dunn, S.; McGrath, J. E. *Polymer* **2008**, *49*, 715.
- (13) Badami, A. S.; Lane, O.; Lee, H.-S.; Roy, A.; McGrath, J. E. *J. Membr. Sci.* **2009**, *333*, 1.
- (14) Nakabayashi, K.; Matsumoto, K.; Ueda, M. *J. Polym. Sci., Polym. Chem.* **2008**, *46*, 3947.
- (15) Mikami, T.; Miyatake, K.; Watanabe, M. *J. Polym. Sci., Polym. Chem.* **2011**, *49*, 452.
- (16) Takamuku, S.; Akizuki, K.; Abe, M.; Kanesaka, H. *J. Polym. Sci., Polym. Chem.* **2009**, *47*, 700.
- (17) Schönberger, F.; Kerres, J. J. *J. Polym. Sci., Polym. Chem.* **2007**, *45*, 5237.
- (18) Lee, H. S.; Lane, O.; McGrath, J. E. *J. Power Sources* **2010**, *195*, 1772.
- (19) Bae, B.; Yoda, T.; Miyatake, K.; Uchida, H.; Watanabe, M. *Angew. Chem., Int. Ed.* **2010**, *49*, 317.
- (20) Bae, B.; Miyatake, K.; Watanabe, M. *Macromolecules* **2010**, *43*, 2684.
- (21) Nakabayashi, K.; Higashihara, T.; Ueda, M. *Macromolecules* **2010**, *43*, 5756.
- (22) Nakabayashi, K.; Higashihara, T.; Ueda, M. *J. Polym. Sci., Polym. Chem.* **2010**, *48*, 2757.
- (23) Takamuku, S.; Jannasch, P. *Macromol. Rapid Commun.* **2011**, *32*, 474.
- (24) Lafitte, B.; Jannasch, P. *Adv. Funct. Mater.* **2007**, *17*, 2823.
- (25) Jutemar, E. P.; Jannasch, P. *J. Membr. Sci.* **2010**, *351*, 87.
- (26) Tian, S.; Meng, Y.; Hay, A. S. *Macromolecules* **2009**, *42*, 1153.
- (27) Zhu, Z.; Walsby, N. M.; Colquhoun, H. M.; Thompson, D.; Petrucco, E. *Fuel Cells* **2009**, *9*, 305.
- (28) Schuster, M.; Kreuer, K. D.; Andersen, H. T.; Maier, J. *Macromolecules* **2007**, *40*, 598.
- (29) Jannasch, P. *Fuel Cells* **2005**, *5*, 248.
- (30) Jutemar, E. P.; Takamuku, S.; Jannasch, P. *Macromol. Rapid Commun.* **2010**, *31*, 1348.
- (31) Ueda, M.; Toyota, H.; Ouchi, T.; Sugiyama, J. I.; Yonetake, K.; Masuko, T.; Teramoto, T. *J. Polym. Sci., Polym. Chem.* **1993**, *31*, 853.
- (32) Wang, F.; Chen, T.; Xu, J. *Macromol. Chem. Phys.* **1998**, *199*, 1421.
- (33) Wang, F.; Li, J.; Chen, T.; Xu, J. *Polymer* **1999**, *40*, 795.
- (34) Buck, E.; Song, Z. J.; Tschaen, D.; Dormer, P. G.; Volante, R. P.; Reider, P. J. *Org. Lett.* **2002**, *4*, 1623.
- (35) Yeager, G. W.; Schissel, D. N. *Synthesis* **1991**, *1*, 63.
- (36) Ben-Haida, A.; Colquhoun, H. M.; Hodge, P.; Lewis, D. F. *Polymer* **1999**, *40*, 5173.
- (37) Ben-Haida, A.; Colquhoun, H. M.; Hodge, P.; Williams, D. J. *J. Mater. Chem.* **2000**, *10*, 2011.
- (38) Colquhoun, H. M.; Paoloni, F. P. V.; Drea, M. G. B.; Hodge, P. *Chem. Commun.* **2007**, 3365.
- (39) Colquhoun, H. M.; Hodge, P.; Paoloni, F. P. V.; McGrail, P. T.; Cross, P. *Macromolecules* **2009**, *42*, 1955.
- (40) Ogata, Y.; Sawaki, Y. *J. Org. Chem.* **1972**, *37*, 2953.
- (41) Syper, L. *Synthesis* **1989**, *3*, 167.
- (42) Jutemar, E. P.; Jannasch, P. *J. Polym. Sci., Polym. Chem.* **2011**, *49*, 734.
- (43) Jutemar, E. P.; Jannasch, P. *ACS Appl. Mater. Interfaces* **2010**, *2*, 3718.
- (44) Daooust, D.; Godard, P.; Devaux, J.; Legras, R.; Strazielle, C. *Polymer* **1994**, *35*, 5491.
- (45) Eisenberg, A.; Kim, J. S. In *Introduction to Ionomers*, 1st ed.; Wiley: New York, 1998.
- (46) Fujimura, M.; Hashimoto, T.; Kawai, H. *Macromolecules* **1981**, *14*, 1309.
- (47) Williams, C. E.; Russel, T. P.; Jerome, R.; Horrion, J. *Macromolecules* **1986**, *19*, 2877.
- (48) Moore, R. B.; Bittencourt, D.; Gauthier, M.; Williams, C. E.; Eisenberg, A. *Macromolecules* **1991**, *24*, 1376.
- (49) Seitz, M. E.; Chan, C. D.; Oppen, K. L.; Baughman, T. W.; Wagener, K. B.; Winey, K. I. *J. Am. Chem. Soc.* **2010**, *132*, 8165.
- (50) Batra, A.; Cohen, C.; Kim, H.; Winey, K. I. *Macromolecules* **2006**, *39*, 1630.
- (51) Guo, R. L.; Lane, O.; VanHouten, D.; McGrath, J. E. *Ind. Eng. Chem. Res.* **2010**, *49*, 12125.